

# Modelling of Laminar Plasma Jet Impinging on a Flatplate with Approximate Box Relaxation Method\*

ZHANG Wen-hong(张文宏), PAN Wen-xia (潘文霞), WU Cheng-kang (吴承康)  
Institute of Mechanics, the Chinese Academy of Sciences, Beijing 100080, China

**Abstract** Approximate Box Relaxation method was used to simulate a plasma jet flow impinging on a flatplate at atmospheric pressure, to achieve a better understanding of the characteristics of plasma jet in materials surface treating. The flow fields under different conditions were simulated and analyzed. The distributions of temperature, velocity and pressure were obtained by modelling. Computed results indicate that this numerical method is suitable for simulation of the flow characteristics of plasma jet, and is helpful for understanding of the mechanism of the plasma-material processing.

**PACS:** 52.65, 52.30

## 1. Introduction

Thermal plasma has been widely used in materials processing since it contains very high energy flux density ( $10^7$ - $10^8$  W/m<sup>2</sup>). The physical parameters of plasma jet such as velocity, temperature and pressure distribution etc. play an important role in the material processing. Knowing these characteristics of the flow field could bring about favorable improvements in controlling the process. However, the very high temperature and complex physical and chemical processes would cause a lot of difficulties in the experimental research on thermal plasma conditions, which handicap further development of plasma technologies in materials processing [1,2]. Thus, numerical simulation becomes an available and effective method for the understanding of plasma processes, along with the development of the computer technologies and the modeling methods [3-5].

Numerical simulation of thermal plasma flow has been used in three aspects: the modeling of arc inside

the plasma generator [3,6], the modeling of plasma flow in a finite chamber [7-9] and the modeling of plasma jet in the infinite space [3, 4, 10]. Relatively fewer papers were involved with plasma jet impinging on a flatplate. Most of these studies made use of the SIMPLE [3,8] algorithm (Patankar 1980) or the commercial CFD code such as the PHOENICS [9].

The Approximate Box Relaxation method [11] (Liu Chaoqun, 1995) is characterized by clear physical concept, simple programming and good stability. Its main consideration is to satisfy the mass conservation law in each control volume during iteration. This method satisfies the conservation law and can be easily used in the multigrid method.

In this paper, The Approximate Box Relaxation method was used to simulate the laminar plasma jet impinging on a flatplate, in order to test its applicability in this area. Distributions of temperature, velocity and pressure under different conditions were

\*Supported by the National Natural Science Foundation of China Project No. 59836220, the Key Project of Chinese Academy of Sciences No. KJ951-1-20, and the Institute of Mechanics President's Foundation.

obtained and analyzed.

## 2. Governing equations.

The time-dependent method was used in this paper, i.e., to solve a steady problem with the method of solving unsteady one. Although this method will spend more CPU time, it has been used widely because of being able to be used in the modelling of unsteady flow on a clear mathematical basis.

The following assumptions were made to formulate the transport equations on the laminar plasma jet impinging on a flatplate [13]:

- (1) The plasma is in local thermodynamic equilibrium (LTE) at atmospheric pressure.
- (2) The flow is symmetrical about the torch axis.
- (3) The temperature, velocity profiles at the exit of the plasma torch are known.
- (4) The arc is optically thin so that radiation may

be accounted for by using an optically thin radiation loss per unit volume.

Based on these assumptions, solutions are sought for a set of elliptical partial differential transport equations that all have the same form:

$$\begin{aligned} & \frac{\partial(\rho\phi)}{\partial t} + \frac{\partial}{\partial x}(\rho u\phi) + \frac{1}{r} \frac{\partial}{\partial r}(r\rho v\phi) \\ & = \frac{\alpha}{\alpha x} \left( \Gamma_\phi \frac{\partial\phi}{\partial x} \right) + \frac{1}{r} \frac{\partial}{\partial r} \left( r\Gamma_\phi \frac{\partial\phi}{\partial r} \right) + S_\phi \end{aligned} \quad (1)$$

Where  $\rho$  is the general variable,  $\Gamma_\phi$  the corresponding diffusion coefficient, and  $S_\phi$  the source term;  $u$  and  $v$  are the axial and radial velocity components,  $\rho$  is the mass density, and  $x$  and  $r$  are the distances in the axial and radial directions respectively. The different terms are given in Table 1 with  $h$  the specific enthalpy,  $\mu$  the laminar viscosity. The gas parameters were taken from the work of Maher, Fauchais and Pfender [12].

Table 1 Terms of the Governing Equations

	$\phi$	$\Gamma_\phi$	$S_\phi$
mass	1	0	0
Axial momentum	$u$	$h$	$\frac{\partial}{\partial x}(\mu \frac{\partial u}{\partial x}) + \frac{1}{r} \frac{\partial}{\partial r}(r\mu \frac{\partial u}{\partial r}) - \frac{\partial p}{\partial x}$
Radial momentum	$v$	$\mu$	$\frac{\partial}{\partial x}(\mu \frac{\partial v}{\partial r}) + \frac{1}{r} \frac{\partial}{\partial r}(r\mu \frac{\partial v}{\partial r}) - 2\mu \frac{v}{r^2} - \frac{\partial p}{\partial r}$
Enthalpy	$h$	$\frac{\mu}{Pr}$	$-Ur$

## 3. Modelling method

The discrete Navier-Stokes equations were derived by means of finite volume approach with diffusion approximated by central difference and convection modeled through hybrid scheme. They were solved with the Approximate Box Relaxation method.

Suppose there are 5 variables  $u_E, u_c, v_N, v_c$  and  $P$  in a control volume (or called as box) as shown in Fig.1, we can write 5 different equations in the cylindrical coordinates:

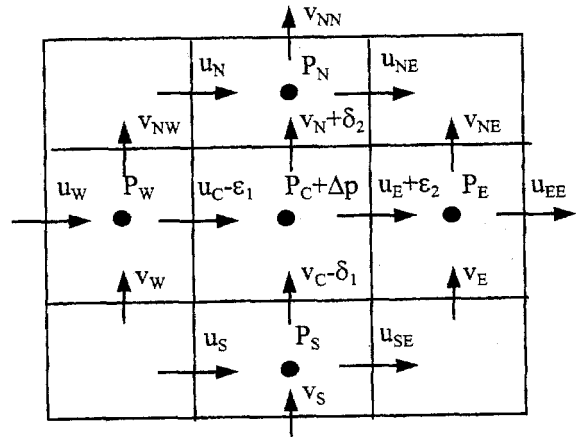


Fig.1 Staggered grid.

$$A_E^C u_E + A_W^C u_W + A_N^C u_N + A_S^C u_S - A_C^C u_C + \frac{P_W - P_C}{\delta x} = S_{u_C}, \quad (2)$$

$$A_E^E u_{EE} + A_W^E u_C + A_N^E u_{NE} + A_S^E u_{SE} - A_C^E u_E + \frac{P_C - P_E}{\delta x} = S_{u_E}, \quad (3)$$

$$B_E^E u_{EE} + B_W^C v_W + B_N^C v_N + B_S^C v_S - B_C^C v_C + \frac{P_S - P_C}{\delta r} = S_{v_C}, \quad (4)$$

$$B_E^N u_{NE} + B_W^N v_{NW} + B_N^N v_{NN} + B_S^N v_{NS} - B_C^N v_N + \frac{P_C - P_N}{\delta r} = S_{v_N}, \quad (5)$$

$$\frac{\rho_E u_E - \rho_C u_C}{\delta x} + \frac{1}{r_C} \frac{r_N \rho_N v_N - r_C \rho_C v_C}{\delta r} = S_\rho, \quad (6)$$

Where:  $A, B$ —coefficients,  $S$ —source terms

There are two steps for the Approximate Box Relaxation method.

$$\begin{cases} (A_E^E \varepsilon_2 + A_C^E \varepsilon_1) - \frac{\Delta P}{\Delta x} = 0 & (A_C^E \varepsilon_2 + A_W^E \varepsilon_1) - \frac{\Delta P}{\Delta x} = 0 \\ (A_E^C \varepsilon_2 + A_C^C \varepsilon_1) - \frac{\Delta P}{\Delta x} = 0 & (A_C^E \varepsilon_2 + A_W^E \varepsilon_1) - \frac{\Delta P}{\Delta x} = 0 \\ \frac{\rho_E \varepsilon_2 - \rho_C \varepsilon_1}{\Delta x} + \frac{1}{r_C} \frac{r_N \rho_N \delta_2 - r_C \rho_C \delta_1}{\Delta r} = S_m \end{cases} \quad (8)$$

Where 
$$S_m = S_\rho - \left( \frac{\rho_E u_e^{old} - \rho_C u_C^{old}}{\Delta x} + \frac{1}{r_C} \frac{r_N \rho_N v_N^{old} - r_C \rho_C v_C^{old}}{\Delta r} \right)$$

Solving equation (8), we get the values of  $\varepsilon_1, \varepsilon_2, \delta_1, \delta_2, \Delta P$ . According to formula (7), new values of the variables are obtained.

Redo the above two steps until the iteration converges.

### 4. Calculation domain and boundary conditions

The calculation domain is sketched in Fig. 2 and the corresponding boundary conditions are given as follows:

#### 1. The first step:

Assume the pressure  $P$  to be a constant; Solve above equations by means of Gauss-Seidel iteration just a few times, so that the velocity  $u$  and  $v$  basically are fit for the above equations.

#### 2. The second step:

Adjust all variables  $u, v$  and  $P$  as follows:

$$\begin{cases} u_C^{new} \leftarrow u_C^{old} - \varepsilon_1, & u_E^{new} \leftarrow u_E^{old} + \varepsilon_2 \\ V_C^{new} \leftarrow V_C^{old} - \delta_1, & V_N^{new} \leftarrow V_N^{old} + \delta_2 \\ P_C^{new} \leftarrow P_C^{old} + \Delta P \end{cases} \quad (7)$$

where, the variables with superscript 'old' present the values before adjusting, 'new' representing the value after adjusting.

Replace the corresponding variable of equation (2)~(5) with the equation (7), since the variables before adjusting basically are fit for equation (2)~(5), we can get the equations:

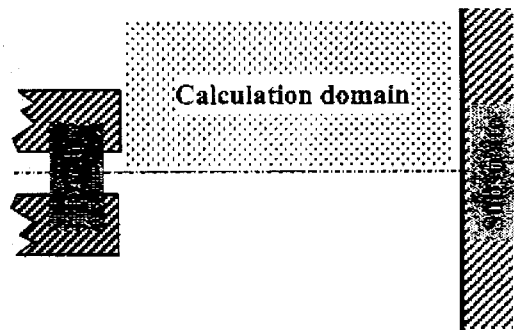


Fig.2 Calculation domain.

(a) Walls (include solid torch exit and substrate)

$$u_W = v_W = 0.$$

$$T_W = 300 \text{ K}$$

(b) Axis of symmetry:

$$v = 0.$$

$$\frac{\partial u}{\partial r} = 0 \quad \frac{\partial p}{\partial r} = 0 \quad \frac{\partial h}{\partial r} = 0$$

(c) Top free boundary:

$$\frac{\partial(\rho vr)}{\partial r} = 0, \quad \frac{\partial u}{\partial r} = 0, \quad \frac{\partial h}{\partial r} = 0$$

(d) Torch nozzle:

The radius of torch nozzle  $R = 0.005$  m, the radial velocity component  $v = 0$ .

The axial velocity and temperature are assumed to have been known:

$$u(r) = u_0 \left[ 1 - \left( \frac{r}{R} \right)^2 \right] \quad u_0 = 200 \text{ m/s}$$

$$T(r) = (T_0 - T_w) \left[ 1 - \left( \frac{r}{R} \right)^2 \right] + T_w \quad T_0 = 10000 \text{ K}$$

## 5. Computed results

(1) Temperature and velocity fields:

Fig.3, Fig.4 and Fig.5 show the simulated results of temperature contours, velocity vector field and streamlines of the laminar plasma jet respectively. These figures shows that the diffusing angle of laminar flow jet is small and the temperature decreases slowly along the axial direction of the plasma jet, compared with a turbulent plasma jet [4,10]. These indicate a greatly reduced exchange of heat and momentum between laminar flow jet and surrounding atmosphere. The shape of the high temperature region in Fig.3 is similar as the appearance of laminar plasma jet in the experiment [14]. This suggests that the modeling method here is suitable for the simulation of the thermal plasma. Moreover, this kind of jet conditions is beneficial for increasing the available efficiency of heat energy and for improving the controlling capability, from the material processing point of view.

(2) The change of temperature and velocity along the centerline for nitrogen and argon:

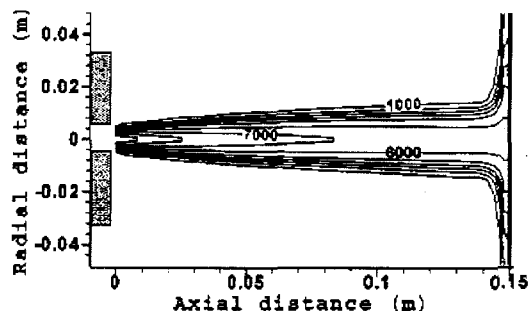


Fig.3 Isotherms of nitrogen plasma jet impinging on a constant temperature flatplate.

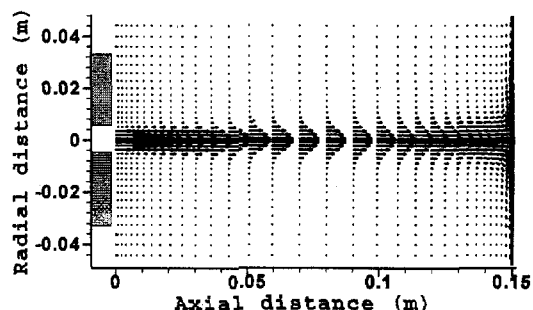


Fig.4 Velocity vector field of nitrogen plasma jet.

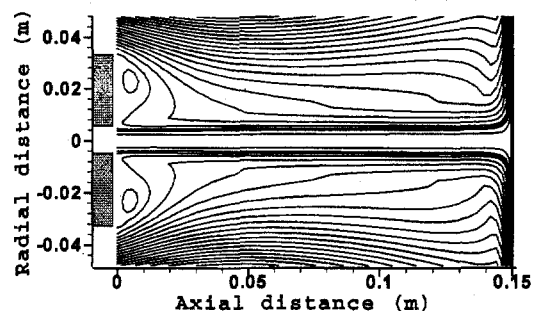


Fig.5 Streamlines of nitrogen plasma jet.

The temperature and velocity distributions along the centerline for nitrogen and argon plasma jets are shown in Fig.6 and Fig.7 respectively. There is an evident difference in the temperature distributions on the axis, because of the different nature of these two gases, even under the same boundary conditions. The temperature of nitrogen plasma jet decreased

much more quickly than that of argon in the vicinity of the torch exit. When the temperature is lower than about 8000K, however, the temperature of nitrogen jet reduced slower than that of argon jet, because the nitrogen enthalpy is higher than argon. The temperature of argon plasma jet decreased to values lower than that of nitrogen jet (Fig.6), when the axial distance is greater than 90mm. This result is in accordance with the experimental observation that the arc jet length of nitrogen plasma is much longer than that of argon. The velocity distributions of the two plasma jets are nearly the same (Fig.7), except that the velocity of nitrogen plasma is a little slower than that of argon plasma. These results could provide a useful reference for the selection of working gas in plasma materials processing.

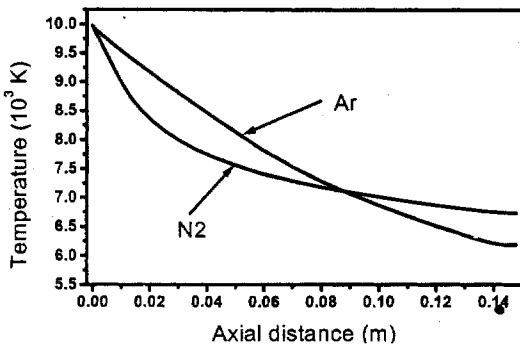


Fig.6 Temperature profiles of nitrogen and argon plasma jet on centerline.

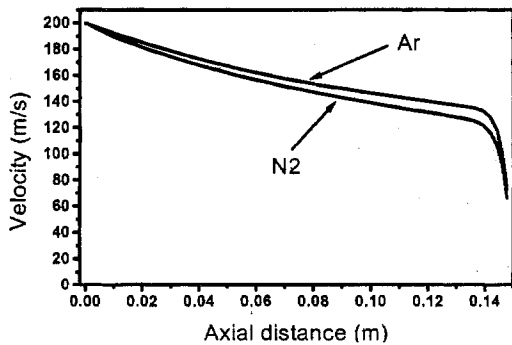


Fig.7 Axial velocity profiles of nitrogen and argon plasma jet on centerline.

(3) Pressure and temperature distribution on the substrate surface: Simulation results showed that the

temperature of jet near the substrate and relative pressure on substrate surface distribution of nitrogen and argon plasma are analogical. Fig.8 shows the relative pressure distributions of nitrogen plasma at different distances between the nozzle and the substrate. The relative pressure varies mainly in the center region. Its value at the stagnation point is inversely proportional to the distance  $L$  (see Fig.8). Temperature distribution of the nitrogen plasma at the cross section 1mm from the substrate is shown in Fig.9. The central temperature decreases with the increase of the nozzle-substrate distance.

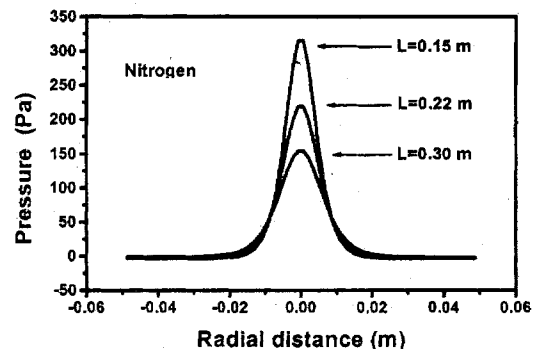


Fig.8 Effect of distance on pressure profiles on the substrate surface.  $L$  is the distance between the nozzle and substrate.

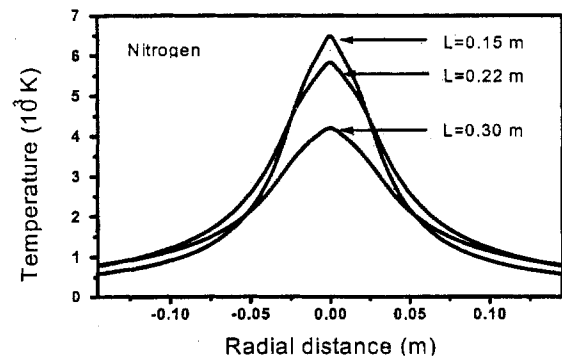


Fig.9 Effect of distance on temperature profiles at the cross section 1 mm off substrate.  $L$  is the distance between the nozzle and substrate.

## 6. Summary

The Approximate Box Relaxation method has been used to solve the governing equations of the plasma flow. Distributions of temperature, velocity and pressure were obtained by the modelling. The results indicate that this numerical method is suitable for simulating the flow characteristics of an arc plasma jet.

## Reference

- [1] O. P. Solonenko, Thermal Plasma and New Material Technology, Cambridge Interscience Publishing, England, (1995).
- [2] R. B. Heimann, Plasma-Spray Coating Principles and Applications, VCH Press, New York, (1996).
- [3] J. M. Bauchire, J. J. Gonzalez, A. Gleizes, Plasma Chemistry and Plasma Processing **17**(1997) 409-432.
- [4] A. H. Dilawari, J. Szekely, Plasma Chemistry and Plasma Processing **7**(1987)317-339.
- [5] M. A. Hedges, R. Taylor, Thermal Spray Research and Applications, Proceedings of the Third National Thermal Spray Conference, USA (1990) 59-63.
- [6] R. Westhoff and J. Szekely, J. Appl. Phys. **70**(1991) 3455-3466.
- [7] H. Nishiyama, T. Saito and S. Kamiyama, Plasma Chemistry and Plasma Processing **16**(1996) 265-286.
- [8] M. F. Agustin, N. Hiroshi et al., J. of Chemical Engineering of Japan **29**(1996) 508-515.
- [9] J. Zierhut, R. Hartmann et al., 14th ISPC Symposium Proceedings, Prague **4** (1999) 2149-2154.
- [10] J. McKelliget, J. Szekely, M. Vardelle and P. Fauchais, Plasma Chemistry and Plasma Processing **2**(1982) 317-332.
- [11] LIU C.Q, Multigrid Methods and its application in numerical fluid dynamics, Tsinghua University Press, Beijing, 1995(in Chinese).
- [12] M.I. Boulos, P. Fauchais and E. Pfender, Plasma Chemistry and Plasma Processing, New York, Vol.1,1994.
- [13] CHEN X., Heat Transfer and Fluid Flow under Thermal Plasma Conditions, Science Press, Beijing, 1993 (in Chinese).
- [14] WU H.C, YANG. X., 13th ISPC Symposium Proceedings, Beijing, **3**(1997)1451-1454.

(Manuscript received 28 September 1999)